

## Comparison of superdeformed bands in $^{61}\text{Zn}$ and $^{60}\text{Zn}$ : Possible evidence for $T=0$ pairing

C.-H. Yu,<sup>1</sup> C. Baktash,<sup>1</sup> J. Dobaczewski,<sup>2</sup> J. A. Cameron,<sup>3</sup> C. Chitu,<sup>4</sup> M. Devlin,<sup>5</sup> J. Eberth,<sup>4</sup> A. Galindo-Uribarri,<sup>1</sup> D. S. Haslip,<sup>3,\*</sup> D. R. LaFosse,<sup>5,†</sup> T. J. Lampman,<sup>3</sup> I.-Y. Lee,<sup>6</sup> F. Lerma,<sup>5</sup> A. O. Macchiavelli,<sup>6</sup> S. D. Paul,<sup>1,7</sup> D. C. Radford,<sup>1</sup> D. Rudolph,<sup>8</sup> D. G. Sarantites,<sup>5</sup> C. E. Svensson,<sup>3,6</sup> J. C. Waddington,<sup>3</sup> and J. N. Wilson<sup>3,5</sup>

<sup>1</sup>Physics Division, Oak Ridge National Laboratory, Oak Ridge, Tennessee 37831

<sup>2</sup>Institute of Theoretical Physics, Warsaw University, Hoża 69, PL-00681 Warsaw, Poland

<sup>3</sup>Department of Physics and Astronomy, McMaster University, Hamilton, Ontario, Canada L8S 4M1

<sup>4</sup>Institut für Kernphysik, Universität zu Köln, D-50937 Köln, Germany

<sup>5</sup>Chemistry Department, Washington University, St. Louis, Missouri 63130

<sup>6</sup>Nuclear Science Division, Lawrence Berkeley National Laboratory, Berkeley, California 94720

<sup>7</sup>Oak Ridge Institute for Science and Education, Oak Ridge, Tennessee 37831

<sup>8</sup>Department of Physics, Lund University, S-22100 Lund, Sweden

(Received 5 May 1999; published 18 August 1999)

The yrast superdeformed band in  $^{61}\text{Zn}$  has been established using  $^{28}\text{Si}(^{36}\text{Ar}, 2pn)^{61}\text{Zn}$  and  $^{40}\text{Ca}(^{29}\text{Si}, 2\alpha)^{61}\text{Zn}$  fusion-evaporation reactions. The excitation energy of this band was determined via two transitions that link this band to the normally deformed states. Lifetime analysis of this band resulted in a quadrupole moment of  $Q_t = 3.0 \pm_{0.4}^{0.5} e b$ , which corresponds to a deformation of  $\beta_2 = 0.50 \pm_{0.06}^{0.07}$ . A comparison of the  $J^{(2)}$  dynamical moments of inertia of the yrast superdeformed band in  $^{61}\text{Zn}$  with those in  $^{60}\text{Zn}$  shows a nearly complete blocking of the observed alignment in  $^{60}\text{Zn}$ , indicating that  $T=0$  proton-neutron pair correlations may be present in  $^{60}\text{Zn}$ . [S0556-2813(99)51109-6]

PACS number(s): 21.10.Re, 21.10.Hw, 23.20.Lv, 27.50.+e

Among the more than 150 established superdeformed (SD) bands [1], the recently discovered [2] SD bands in the mass  $A \sim 60$  region are unique for two reasons. First, they belong to the lightest mass region where superdeformation has been observed. Therefore, they exhibit the highest rotational frequencies. Second, superdeformed nuclei in this mass region are self-conjugate or nearly self-conjugate. This allows the investigation of isospin-sensitive properties in SD nuclei for the first time. Our recent study [3] of the SD band in the  $N=Z$  nucleus  $^{60}\text{Zn}$  has shown two interesting phenomena: (i) The SD band decays out by stretched- $E2$  transitions, suggesting that the process may be nonstatistical; and (ii) the  $J^{(2)}$  dynamical moments of inertia exhibit a large rise at low angular frequency, which has been interpreted as the simultaneous alignment of two pairs of  $g_{9/2}$  protons and neutrons. In  $^{62}\text{Zn}$  [2], the decay-out transitions of the SD band were not established, possibly indicating a different decay-out process compared to that in  $^{60}\text{Zn}$ . This suggests that additional neutrons outside the  $N=30$  SD shell gap may significantly affect both pair correlations and the barrier between the SD and normally deformed (ND) potential wells. To further understand these issues, it is important to study  $^{61}\text{Zn}$ , which has only one neutron outside the  $N=30$  SD shell gap and, thus, could provide information on pair correlations, as well as on other nuclear properties sensitive to changing valence particles.

High-spin states in  $^{61}\text{Zn}$  were populated in two experiments performed at the Lawrence Berkeley National Labo-

ratory. In both experiments,  $\gamma$  rays were detected by the Gammasphere array [4] (comprising of 82 and 100 Compton suppressed Ge detectors in the first and second experiments, respectively), and evaporated charged particles were detected by the 95-element CsI detector array Microball [5]. The charged particle information was used to select the reaction channel and to determine the velocity vector of the recoil. The SD band in  $^{61}\text{Zn}$  was identified from the analysis of the channel-selected  $\gamma\gamma\gamma$  cubes from the two reactions. Figure 1 shows a level scheme of this band and the ND states [6,7] in  $^{61}\text{Zn}$ .

*Results from the first experiment.* About 250 million 2-proton-gated,  $\gamma\gamma$  or higher fold events, were obtained from the  $^{28}\text{Si}(^{36}\text{Ar}, 2pn)$  reaction at a beam energy of 143 MeV. The target consisted of a layer of  $0.42 \text{ mg/cm}^2$  isotopically enriched  $^{28}\text{Si}$  evaporated onto a  $0.9 \text{ mg/cm}^2$  Ta foil, which faced the beam. The SD band, established up to the 3127-keV transition, was observed to decay to the ND states via two linking transitions (5127- and 5278-keV), as shown in Fig. 1 and the inset of Fig. 2(a).

To determine the multipolarities of the observed transitions, data were summed up for the 15 most backward-angle detectors ( $142.6^\circ$ ,  $148.3^\circ$ , and  $162.7^\circ$ ) and 25 detectors near  $90^\circ$  ( $79.2^\circ$ ,  $80.7^\circ$ ,  $90.0^\circ$ ,  $99.3^\circ$ , and  $100.8^\circ$ ) to form two groups labeled as “ $30^\circ$ ” and “ $83^\circ$ ,” respectively. (The labels represent the effective angles corresponding to the averaged cosines of the two detector groups.) A  $30^\circ$  versus  $83^\circ$  matrix was created from a subset of  $\gamma\gamma\gamma$  events, each having at least one  $\gamma$  ray identified as a known  $^{61}\text{Zn}$  transition. From this matrix, information of directional correlations from oriented states (DCO) was then obtained by extracting DCO ratios defined as

$$\frac{I(30^\circ)}{I(83^\circ)}(\gamma_1) = \frac{I(\gamma_1 \text{ at } 30^\circ, \text{ gated with } \gamma_2 \text{ at } 83^\circ)}{I(\gamma_1 \text{ at } 83^\circ, \text{ gated with } \gamma_2 \text{ at } 30^\circ)} \quad (1)$$

\*Present address: Defense Research Establishment Ottawa, Ottawa, Ontario, Canada K1A 0Z4.

†Present address: Dept. of Physics, State University of New York at Stony Brook, Stony Brook, NY 11794.

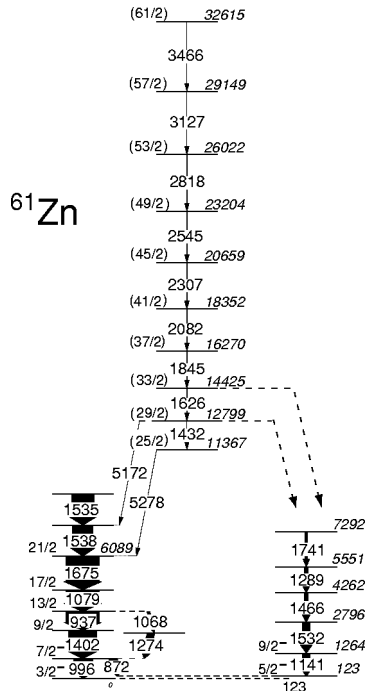


FIG. 1. Level scheme of the SD band in  $^{61}\text{Zn}$  deduced from the present work. The errors of the transition energies are about 1–2 keV for the SD band, and 3–4 keV for the 5172- and 5278-keV linking transitions. See text for details of spin and parity assignments.

and are plotted in Fig. 3 for both the SD band and some ND states. When compared to the known [6]  $E2$  and dipole transitions (open symbols), Fig. 3 shows that the 937-, 1079-, and 1675-keV transitions are quadrupole transitions, whereas the 1402-keV transition is a dipole transition. If all the quadrupole transitions are stretched  $E2$  transitions, the spins of these ND levels can be assigned as shown in Fig. 1. The DCO ratio for the 5278-keV linking transition has very large error bars, but slightly favors the quadrupole character (see Fig. 3). An assumption of stretched  $E2$  character for this transition (which makes the decay-out pattern similar to that in  $^{60}\text{Zn}$ ), along with the clear quadrupole character for the transitions in the SD band (see Fig. 3) results in the spin assignments shown in parentheses in Fig. 1.

In addition to the observed linking transitions, the SD band also decays out at spins (33/2) and (29/2) to another set of ND states (see Fig. 1). The linking transitions themselves, however, were not established. The relative intensity of the SD band is shown as the inset in Fig. 2(b). The total intensity of the SD band is approximately 1.6% of that of the 937-keV (ND) transition. The 5278-keV decay-out transition carries about 25% of the intensity of the 1432-keV (SD) transition, and the branching ratio for the 5172-keV transition is <25%.

*Results from the second experiment.* About 64 million  $2\alpha$ -gated,  $\gamma\gamma$  or higher fold events, were obtained from the  $^{40}\text{Ca}(^{29}\text{Si}, 2\alpha)$  reaction at a beam energy of 130 MeV. The target consisted of a layer of  $0.5\text{ mg/cm}^2$  enriched  $^{40}\text{Ca}$  evaporated onto a layer of  $2.5\text{ mg/cm}^2$  Ta foil as backing. The SD band in  $^{61}\text{Zn}$  was observed one level higher than in

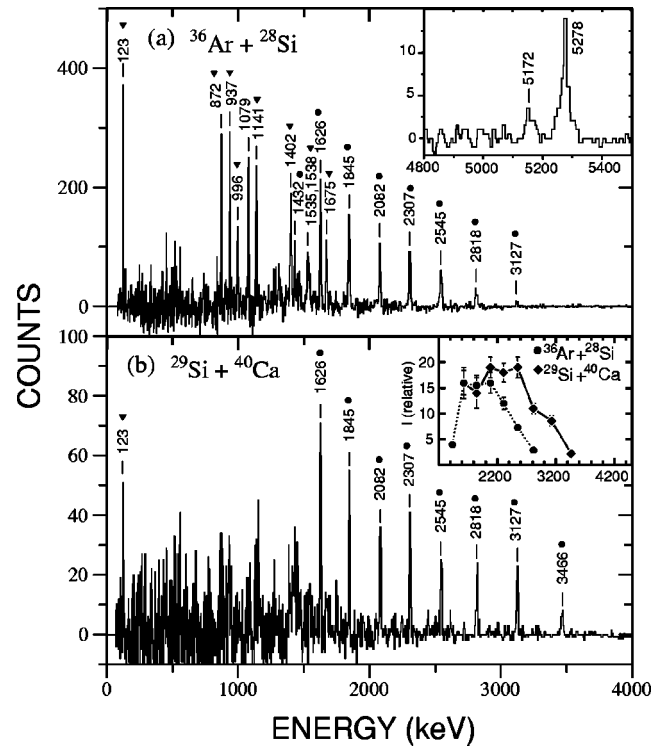


FIG. 2. (a) Spectrum obtained by summing all possible double gates on members of the SD band in  $^{61}\text{Zn}$  from the  $^{28}\text{Si}(^{36}\text{Ar}, 2pn)$  reaction. Circles and triangles represent the SD band and low-spin ND states in  $^{61}\text{Zn}$ , respectively. The inset shows the two transitions that connect the SD band to the ND band. (b) Similar spectrum obtained from the  $^{40}\text{Ca}(^{29}\text{Si}, 2\alpha)$  reaction. Most transitions from ND states are broadened due to the Ta backing. The inset shows the relative intensities of the SD band from both reactions. The two curves are normalized at 1626 keV, with the y axis representing the percentage of intensities relative to the 937-keV transition ( $=1000$ ) from the  $^{28}\text{Si}(^{36}\text{Ar}, 2pn)$  reaction.

the  $^{36}\text{Ar}+^{28}\text{Si}$  reaction [see Figs. 1 and 2(b)]. This is consistent with the relative intensity patterns of the SD band from the two reactions [see inset of Fig. 2(b)], and suggests that the feeding of the SD band occurred at a higher spin for the  $^{29}\text{Si}+^{40}\text{Ca}$  reaction than for the  $^{36}\text{Ar}+^{28}\text{Si}$  reaction. The 5172- and 5278-keV decay-out transitions were also observed in this reaction.

A search for possible discrete-line proton decays [8,9] from the SD band was unsuccessful in both experiments. An analysis of coincidence intensities between the SD band and the 996-, 872-, and 1141-keV ND transitions established an upper limit of  $\sim 5\%$  for the missing  $\gamma$  intensity that might be attributed to such a decay mode.

Since the dipole 1402-keV transition can be either  $E1$  or  $M1$ , the parities of the higher spin ND and SD states cannot be determined. Furthermore, although the DCO ratio of the 5278-keV linking transition favors the  $E2$  assignment, its large uncertainties could not rule out  $E1$  or  $M1$  assignments, see Fig. 3. Thus, the 11367-keV SD level is likely to have  $I=25/2$ , corresponding to the signature index of  $\alpha=+1/2$ . But a spin assignment of  $I=23/2$  ( $\alpha=-1/2$ ) cannot be ruled out. The parity of the band is uncertain in either of the two scenarios.

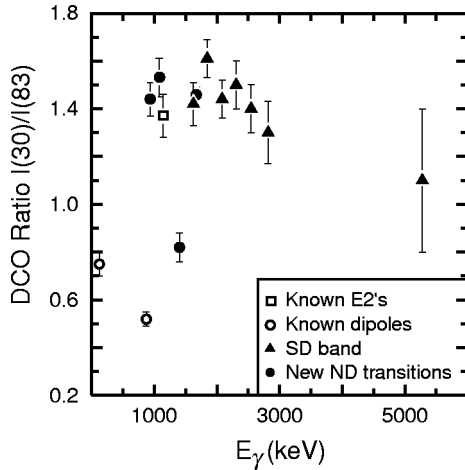


FIG. 3. DCO ratios,  $I(30^\circ)/I(83^\circ)$ , as a function of  $\gamma$ -ray energy for transitions in  $^{61}\text{Zn}$ . The “known” multiplicities refer to the results from the previous measurement [6]. See text for a more detailed description.

The average transition quadrupole moment  $Q_t$  of the SD band in  $^{61}\text{Zn}$  was measured with data from the  $^{28}\text{Si}(^{36}\text{Ar}, 2pn)$  reaction. Using the technique described in Refs. [10,11], the relative velocity of the recoils,  $F_\tau = v(E_\gamma)/v_{\text{max}}$ , were extracted for the SD band and shown in Fig. 4 together with calculations. For comparison, the  $F_\tau$ 's of several low spin ND states are also plotted (diamonds). The calculations used the LINESHAPE program [12] and the stopping powers in Ref. [13] (corrected according to Ref. [14]). The simulations used a time step of 0.7 fs and produced 1000 histories. Side feedings were modeled by a two-level rotational sequence into each state with the same  $Q_t$  and  $J^{(2)}$  as the SD band. The uncertainty associated with these assumptions is not included in the final results, but is expected to be much smaller than the shown errors. The best fit between the experimental and calculated  $F_\tau$ 's resulted in a  $Q_t = 3.0 \pm_{0.4}^{0.5} e b$  for the SD band in  $^{61}\text{Zn}$  [see Fig. 4(a)]. Assuming an axially symmetric shape, this corresponds to a quadrupole deformation of  $\beta_2 = 0.50 \pm_{0.06}^{0.07}$ . This result is compared to the calculated ones in Fig. 4(b).

Calculations of the SD bands in  $^{61}\text{Zn}$  have been performed within the Hartree-Fock (HF) method (no pairing) with the Skyrme SLy4 interaction [15], using the code HFODD (v1.75) [16]. Detailed analysis of the SD bands in this mass region will be published elsewhere [17]. The SD configurations in  $^{61}\text{Zn}$  are built on the doubly magic  $4^2 4^2$  SD configuration in  $^{60}\text{Zn}$ . ( $4^n 4^p$  denotes that  $n$  and  $p$  lowest  $g_{9/2}$   $N_0 = 4$  intruder states are occupied for neutrons and protons, respectively.) Above the  $Z = 30$  SD gap, the 31st neutron in  $^{61}\text{Zn}$  can occupy five possible orbitals, which are (a) the third intruder state  $[431]3/2(\alpha = +1/2)$ , which gives the  $4^3 4^2$  configuration; and (b) the two signatures of the  $[310]1/2$  or  $[303]7/2$  orbitals, which correspond to the  $4^2 4^2$  configurations.

Among the above five possible assignments for the SD band in  $^{61}\text{Zn}$ , the two high- $K$  configurations ( $[303]7/2$ ) are least likely, because they correspond to two strongly-coupled signature partners that lie close to each other, and both

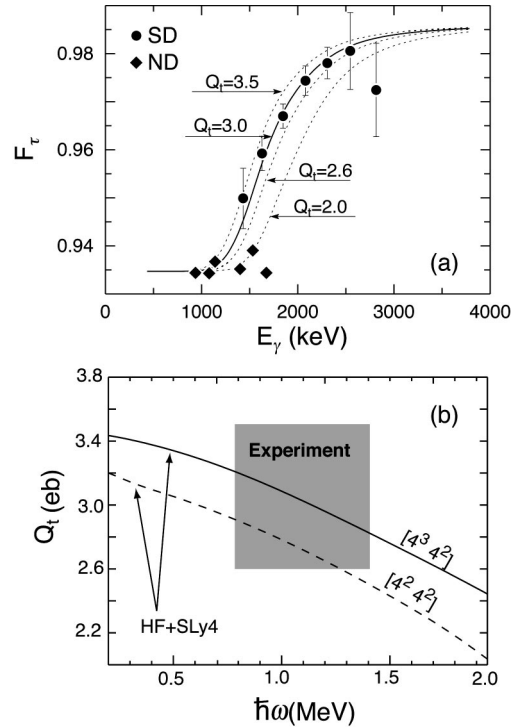


FIG. 4. (a) Experimental (filled symbols) and calculated (curves) values of  $F_\tau$  as functions of  $E_\gamma$  for the SD (circles) and some ND (diamonds) transitions in  $^{61}\text{Zn}$ . (b) Calculated (HF + SLy4)  $Q_t$ 's as a function of  $\hbar\omega$  for the SD band in  $^{61}\text{Zn}$ . Solid and dashed lines correspond to the  $[431]3/2(\alpha = +1/2)$ ,  $[4^3 4^2]$  and  $[310]1/2(\alpha = +1/2)$ ,  $[4^2 4^2]$  configurations, respectively. The shaded area represents the measured  $Q_t$  with its height indicating the experimental uncertainty, and its width indicating the region of  $\hbar\omega$  where experimental data were available for measurement.

should have been observed experimentally (see, e.g., ND bands in  $^{62}\text{Zn}$  [18]). No evidence for the presence of the signature partner of the observed SD band in  $^{61}\text{Zn}$  was found in our experiments. The  $[310]1/2(\alpha = -1/2)$  assignment is also unlikely, because it is calculated to lie about 0.5 MeV higher than its opposite-signature band  $[310]1/2(\alpha = +1/2)$ , and thus is energetically unfavored. The remaining two configurations, namely,  $[431]3/2(\alpha = +1/2)$ ,  $[4^3 4^2]$  and  $[310]1/2(\alpha = +1/2)$ ,  $[4^2 4^2]$ , have opposite parities but the same signature  $\alpha = +1/2$ , and thus are in good agreement with the most likely signature assignment based on experimental DCO ratios. To further narrow down the choice between these two options, we have examined the calculated quadrupole moments  $Q_t$  [Fig. 4(b)], dynamic moments of inertia,  $J^{(2)}$  [Fig. 5(a)], and the relative alignments  $\Delta I$  with respect to the SD band in  $^{58}\text{Cu}$  [Fig. 5(b)]. The experimental data agree better with the calculated results for the  $4^3 4^2$  configuration than those for the  $4^2 4^2$  assignment. The very good agreement of the calculated  $J^{(2)}$  and  $\Delta I$  with the experimental data at high  $\hbar\omega$  for the  $4^3 4^2$  configuration is especially convincing, because ( $T = 1$ ) pair correlations are least important at high spins.

The experimental  $J^{(2)}$  moments of inertia for the SD band in  $^{61}\text{Zn}$  are plotted in Fig. 6 together with those in  $^{60,62}\text{Zn}$ . The most pronounced feature seen in Fig. 6 is the peaking of

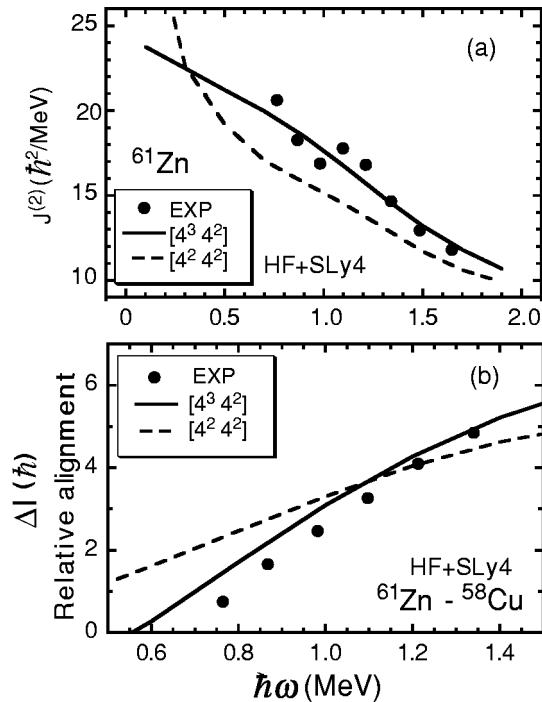


FIG. 5. (a) Experimental (filled circles) and theoretical (curves) dynamic moments of inertia,  $J^{(2)}$ , of the SD band in  $^{61}\text{Zn}$ . (b) Experimental (filled circles) and theoretical (curves) relative alignments of the SD band in  $^{61}\text{Zn}$  ( $I=25/2$  was assumed for the 11367-keV level) with respect to those of the SD band in  $^{58}\text{Cu}$  [9] ( $I=9$  was assumed for the 8915-keV level). Solid and dashed lines correspond to the  $[431]3/2(\alpha=+1/2)$  and  $[310]1/2(\alpha=+1/2)$  configurations, respectively. The  $^{58}\text{Cu}$  band was chosen as the reference, because it is free of discontinuities and can be well described by calculations [9], which is not the case for the  $^{60}\text{Zn}$  reference.

$J^{(2)}$  at low spin in  $^{60}\text{Zn}$ , and the absence of a similar peak in  $^{61}\text{Zn}$  (data for  $^{62}\text{Zn}$  are not sufficient to either rule out or establish such a peak). The peak in  $^{60}\text{Zn}$  has been interpreted [3] as the simultaneous alignments of the  $g_{9/2}$  protons and neutrons. This interpretation is now difficult to understand in view of the absence of any alignment gain in  $^{61}\text{Zn}$  that might be attributed to the  $g_{9/2}$  orbitals. If independent proton-

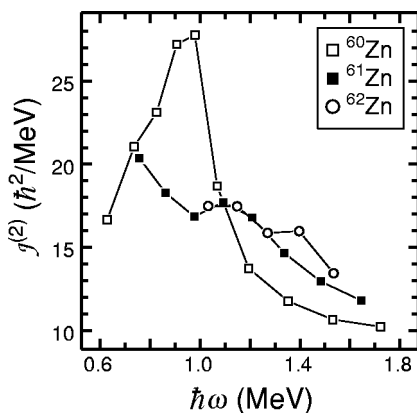


FIG. 6. Experimental  $J^{(2)}$  moments of inertia for the SD bands in  $^{60,61,62}\text{Zn}$ . Data for  $^{60,62}\text{Zn}$  are from Refs. [2,3].

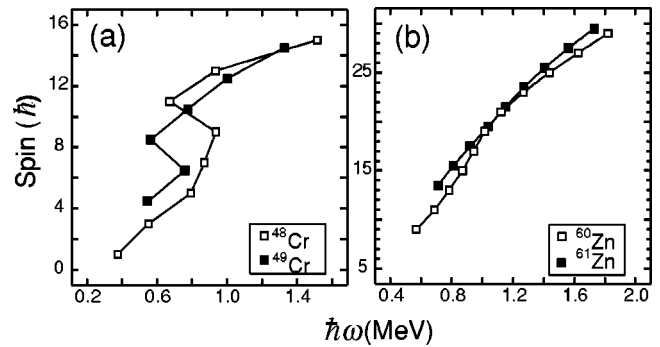


FIG. 7. (a) Spin as function of  $\hbar\omega$  in the yrast bands of  $^{48,49}\text{Cr}$  compared to (b) those of the SD bands in  $^{60,61}\text{Zn}$ .

proton ( $p$ - $p$ ) and neutron-neutron ( $n$ - $n$ ) pair correlations were responsible for the simultaneous proton and neutron alignments in  $^{60}\text{Zn}$ , the odd neutron in  $^{61}\text{Zn}$  should only block the neutron contribution to the alignment, while the proton part should remain and should result in an alignment roughly half of that observed in  $^{60}\text{Zn}$ . The only noticeable bump in the  $J^{(2)}$  plot of  $^{61}\text{Zn}$  in Fig. 6 occurs at a higher  $\hbar\omega$  of  $\sim 1.1$  MeV, and the alignment gain is much too small to be attributed to the  $g_{9/2}$  proton pair.

The anomalous behavior of this crossing is best seen when it is compared with the example of simultaneous alignments of neutrons and protons in the  $N=Z$  nucleus  $^{48}\text{Cr}$  [19]. The spins of the yrast band in this nucleus are plotted as a function of  $\hbar\omega$  in Fig. 7(a) together with those for  $^{49}\text{Cr}$  [20]. Here the role played by the odd neutron in  $^{49}\text{Cr}$  is obvious: With the neutron alignment blocked in  $^{49}\text{Cr}$ , its total alignment is half of that in  $^{48}\text{Cr}$ . At the lowest and highest  $\hbar\omega$ , the spins of  $^{49}\text{Cr}$  are, respectively, larger and smaller than the spins of  $^{48}\text{Cr}$ . Such a pattern is not seen in the pair of SD nuclei  $^{60}\text{Zn}$  and  $^{61}\text{Zn}$  [see Fig. 7(b)]. The spins of  $^{61}\text{Zn}$  are larger than those in  $^{60}\text{Zn}$  both at low and high angular frequencies.

The observed peak in  $^{60}\text{Zn}$  is unlikely to be the result of a simple single-particle like evolution of the structure, such as an unpaired crossing that has been observed in  $^{147}\text{Gd}$  [21]. This is because in a doubly magic SD system (such as  $^{60}\text{Zn}$ ), there are no candidate orbitals for such a crossing. Furthermore, even if such a crossing were present, it should occur for both neutrons and protons in the  $N=Z$  nucleus  $^{60}\text{Zn}$ , and should have persisted for protons in  $^{61}\text{Zn}$ . Therefore, in the absence of any conventional explanation for the observed anomaly, one has to consider alternative mechanisms.

We would like to offer a tentative explanation to this anomaly in terms of a change in the pairing correlations. Although it is known that Coriolis antipairing significantly reduces the conventional ( $T=1$ ), static  $p$ - $p$  and  $n$ - $n$  pairing correlations at very high spins, the  $T=0$  proton-neutron ( $p$ - $n$ ) correlations are not necessarily destroyed by rotation. Therefore, the absence of the expected alignment in  $^{61}\text{Zn}$  may indicate that the peak in the  $J^{(2)}$  of  $^{60}\text{Zn}$  is due to the crossing of the  $T=1$  and  $T=0$  bands. (The addition of one neutron to  $^{60}\text{Zn}$  would significantly reduce the  $T=0$   $p$ - $n$  correlations in  $^{61}\text{Zn}$ .) Obviously, more experimental and, specially, theoretical investigations of properties of odd- and

odd-odd nuclei around  $^{60}\text{Zn}$  are needed to support or disprove such a hypothesis. Unfortunately, despite intense theoretical investigations of the competition between the  $T=1$  and  $T=0$  pairing modes, a satisfactory description of this problem is still lacking. However, a recent calculation of high-spin properties of  $^{48}\text{Cr}$  indicates that the  $T=0$  mode may indeed survive at high frequencies where the  $T=1$  mode has been quenched [22]. Similar calculations in  $^{60}\text{Zn}$  are not yet available. In view of the results discussed here, it is highly desirable to perform self-consistent, particle- and isospin-projected calculations that would treat the  $T=1$  and  $T=0$  pairing modes on equal footing.

To summarize, the yrast superdeformed band in the  $N=Z+1$  nucleus  $^{61}\text{Zn}$  was established using two complementary reactions. Two discrete transitions linking this SD band to the normally deformed states were observed, which are probably  $E2$  transitions. Experimental evidence as well as theoretical calculations show that this band most likely has the  $[\nu g_{9/2}]^3[\pi g_{9/2}]^2$  configuration. The measured quadrupole moment of  $Q_t=3.0\pm_{0.4}^{0.5}e$  corresponds to  $\beta_2=0.50$

$\pm_{0.06}^{0.07}$ , which is consistent with the tentative configuration assignment. Comparisons of the  $J^{(2)}$  moments of inertia and relative spins of the SD bands in  $^{61}\text{Zn}$  and  $^{60}\text{Zn}$  show in  $^{61}\text{Zn}$  the absence of an alignment observed in  $^{60}\text{Zn}$ , suggesting that the effect in  $^{60}\text{Zn}$  may be caused by a different mechanism than the simultaneous alignment of neutrons and protons. An alternative explanation that stipulates the presence of  $T=0$  proton-neutron pairing correlations in  $^{60}\text{Zn}$  may provide a solution to this anomaly.

Fruitful discussions with Dr. R. Wyss are gratefully acknowledged. Oak Ridge National Laboratory is managed by Lockheed Martin Energy Research Corp. for the U.S. DOE under Contract No. DE-AC05-96OR22464. This work was also supported by the U.S. DOE [Contract Nos. DE-AC05-76OR00033 (ORISE) and DE-FG05-88ER40406(WU)], the Polish CSR (Contract No. 2 P03B 040 14), the German BMBF (Contract No. 06-OK-862I), the National Science and Engineering Research Council of Canada, and the Swedish Natural Science Research Councils.

- 
- [1] X.-L. Han *et al.*, At. Data Nucl. Data Tables **63**, 117 (1996); X.-L. Han *et al.* (unpublished).
- [2] C.E. Svensson *et al.*, Phys. Rev. Lett. **79**, 1233 (1997).
- [3] C.E. Svensson *et al.*, Phys. Rev. Lett. **82**, 3400 (1999).
- [4] I.Y. Lee, Nucl. Phys. **A520**, 641c (1990).
- [5] D.G. Sarantites *et al.*, Nucl. Instrum. Methods Phys. Res. A **381**, 418 (1996).
- [6] R.B. Schubank *et al.*, Phys. Rev. C **40**, 2310 (1989).
- [7] S.M. Vincent *et al.*, J. Phys. G **25**, 941 (1999).
- [8] C. Chitu *et al.* (unpublished).
- [9] D. Rudolph *et al.*, Phys. Rev. Lett. **80**, 3018 (1998).
- [10] B. Cederwall *et al.*, Nucl. Instrum. Methods Phys. Res. A **354**, 591 (1995).
- [11] C.-H. Yu *et al.*, Phys. Rev. C **57**, 113 (1998).
- [12] J.C. Wells *et al.*, "LINESHAPE: A Computer Program for Doppler Broadened Lineshape Analysis," Report No. ORNL-6689 ORNL Physics Division Prog. Rep. 30, 1991, p.44.
- [13] L.C. Northcliffe and R.F. Schilling, Nucl. Data Tables **7**, 256 (1970).
- [14] J.F. Ziegler and W.K. Chu, At. Data Nucl. Data Tables **13**, 463 (1974).
- [15] E. Chabanat *et al.*, Nucl. Phys. **A635**, 231 (1998).
- [16] J. Dobaczewski and J. Dudek, Comput. Phys. Commun. **102**, 166 (1997); **102**, 183 (1997); (unpublished).
- [17] J. Dobaczewski, W. Satuła, W. Nazarewicz, and C. Baktash (unpublished).
- [18] C.E. Svensson *et al.*, Phys. Rev. Lett. **80**, 2558 (1998).
- [19] S.M. Lenzi *et al.*, Z. Phys. A **354**, 117 (1996); J.A. Cameron *et al.*, Phys. Lett. B **387**, 266 (1996).
- [20] J.A. Cameron *et al.*, Phys. Lett. B **235**, 239 (1990); C.D. O'Leary *et al.*, Phys. Rev. Lett. **79**, 4349 (1997).
- [21] C. Theisen *et al.*, Phys. Rev. C **54**, 2910 (1996), and references therein.
- [22] J. Terasaki, R. Wyss, and P.-H. Heenen, Phys. Lett. B **437**, 1 (1998).